The expression of $\tilde{\mathbf{h}}_f(l)$ can be obtained by performing inverse z-transform on $\mathbf{T}_f(z)\cdot\underline{\tilde{\mathbf{h}}}(0)$. After some manipulation, with a carefully selected α and μ, $\tilde{\mathbf{h}}_f(l) \to 0$ when $l \to \infty$, i.e. the MSTE of the SOLMS-based tracking defined as $MSTE = E_{l\to\infty}\left[\tilde{\mathbf{h}}^H(l)\cdot\tilde{\mathbf{h}}(l)\right]$ can be computed as

$$MSTE = \underset{l\to\infty}{E}\left[\tilde{\mathbf{h}}_N^H(l)\cdot\tilde{\mathbf{h}}_N(l)\right] + \underset{l\to\infty}{E}\left[\tilde{\mathbf{h}}_T^H(l)\cdot\tilde{\mathbf{h}}_T(l)\right] \quad (6)$$

We name the first term in the right-hand side of eqn. 6 as $MSTE_N$, and the second term as $MSTE_T$. Given σ_n^2 and $s_m(\omega)$, either $MSTE_N$ or $MSTE_T$ can be expressed as a function of α and μ in the frequency domain

$$MSTE_N = \sum_{m=1}^{2}\frac{1}{2\pi}\int_{-\pi}^{\pi}\left|T_{N,m}(e^{j\omega})\right|^2\cdot 0.5\cdot\sigma_n^2\cdot d\omega \quad (7)$$

$$MSTE_T = \sum_{m=1}^{2}\frac{1}{2\pi}\int_{-\pi}^{\pi}\left|T_{T,m}(e^{j\omega})\right|^2\cdot s_m(\omega)\cdot d\omega \quad (8)$$

where $T_{N,m}(z)$ and $T_{T,m}(z)$ are the m_{th} diagonal element of $\mathbf{T}_N(z)$ and $\mathbf{T}_T(z)$, respectively. Therefore, provided that σ_n^2 and $s_m(\omega)$ are available, we can take eqn. 6 as the objective function and obtain the optimum α and μ with numerical optimisation methods.

Specially, we consider the situation where $h_m(l)$ is described by the Jake's fading channel model [3]:

$$s_m(\omega) = \begin{cases}\frac{2}{\omega_D}\left[1-\left(\frac{\omega}{\omega_D}\right)^2\right]^{-1/2} & -\omega_D < \omega < \omega_D \\ 0 & \text{otherwise}\end{cases} \quad (9)$$

Table 1 shows the optimised α and μ for some settings of ω_D and $SNR = 10\cdot\log_{10}(1/\sigma_n^2)$, together with corresponding MSTE. For comparison, Table 1 also shows the optimum MSTE achieved by the optimum LMS-based tracking method developed in [3]. The comparison shows that the superiority of the SOLMS-based method is quite distinct.

Table 1: Optimum parameters and performance comparison

ω_D	2.6×10^{-3}			4.7×10^{-2}		
SNR (dB)	10	15	20	10	15	20
μ	0.026	0.032	0.040	0.254	0.301	0.359
α	0.013	0.016	0.020	0.126	0.163	0.209
MSTE1 (dB)	−21.94	−25.94	−29.94	−11.50	−15.44	−19.34
MSTE2 (dB)	−19.14	−22.48	−25.81	−10.78	−14.11	−17.44

MSTE1 is performance of SOLMS algorithm
MSTE2 is performance of LMS algorithm

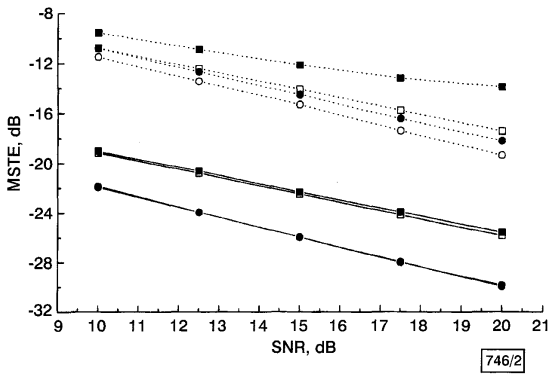

Fig. 2 *MSTE against SNR*

slow $\omega_D = 2.6\times10^{-3}$
fast $\omega_D = 4.7\times10^{-2}$
—■— $MSTE_{MC}$ of LMS (slow)
—□— analytical MSTE of LMS (slow)
—●— $MSTE_{MC}$ of SOLMS (slow)
—○— analytical MSTE of SOLMS (slow)
····■···· $MSTE_{MC}$ of LMS (fast)
····□···· analytical MSTE of LMS (fast)
····●···· $MSTE_{MC}$ of SOLMS (fast)
····○···· analytical MSTE of SOLMS (fast)

Simulation results: We support our development with Monte-Carlo simulations. The independent complex fading gains $\{h_1(l), h_2(l)\}$ are generated with the algorithm in [4] and independent QPSK sequences are used as $c_1(l)$ and $c_2(l)$. Each transmission burst consists of 1500 symbols and the first two symbols are used as pilots, with which a noise contaminated $\hat{\mathbf{h}}(0)$ is obtained. Fig. 2 shows the simulation results, where

$$MSTE_{MC} = E\left[\frac{1}{1000}\sum_{l=500}^{1500}\sum_{m=1}^{2}|h_m(l)|^2\right]$$

and $E[\cdot]$ is obtained as the average of 400 independent trials. From Fig. 2 it can be seen that the proposed optimum SOLMS-based wireless channel tracking offers a quite distinct benefit over the LMS-based method, although the 'absolute' analytical results seem to be a little too optimistic in the fast fading channels.

Conclusions: We have developed optimum SOLMS-based wireless channel tracking with the aid of a frequency domain analysis. Simulation results show that the proposed methods can offer quite distinct benefit in comparison with the LMS based method.

21 May 2001
Electronics Letters Online No: 20010656
DOI: 10.1049/el:20010656

Yisheng Xue and Xuelong Zhu (*Department of Electronic Engineering, TsingHua University, Beijing, 100084, People's Republic of China*)

E-mail: xueys@mails.tsinghua.edu.cn

References

1 GAZOR, S.: 'Prediction in LMS-type adaptive algorithms for smoothly time varying environments', *IEEE Trans. Signal Process.*, 1999, **47**, (6), pp. 1735–1739
2 SHAHTALEBI, K., GAZOR, S., PASUPATHY, S., and GULAK, P.G.: 'Second-order H^∞ optimal LMS and NLMS algorithms based on a second-order Markov model', *IEE Proc., Vis. Image Signal Process.*, 2000, **147**, (3), pp. 231–237
3 LIN, J., PROAKIS, J.G., LING, F., and LEV-ARI, H.: 'Optimal tracking of time-varying channels: a frequency domain approach for known and new algorithms', *IEEE J. Sel. Areas Commun.*, 1995, **13**, (1), pp. 141–154
4 SMITH, J.I.: 'A computer generated multipath fading simulation for mobile radio', *IEEE Trans. Veh. Technol.*, 1975, **24**, (3), pp. 39–40

Recursive digital filter for fast visual evoked potential estimation and classification

R. Palaniappan and P. Raveendran

Generally, visual evoked potential (VEP) estimation requires power spectrum computation. Here VEP is estimated using a recursive digital filter, which is faster and simpler to design. The method assumes VEP can be represented by a 40 Hz spectrum and the filter extracts a 40 Hz signal in the time domain, circumventing the normal procedure of power spectrum computation. Experimental results validate the method for discriminating alcoholics from control subjects.

Introduction: Visual evoked potential (VEP) are signals generated in the brain in response to visual stimulus. Analysis of VEP, using power spectrum, has become very useful for neuropsychological studies and clinical purposes. However, spectral computation using classical Fourier methods or parametric methods such as autoregressive is time consuming and requires proper selection of windows, model order, etc. We propose a faster method that circumvents spectral computation for VEP estimation. This method is also simpler and cost efficient to design using microprocessors. The method assumes that VEP signals can be represented by 40 Hz spectra, since studies in [1,2] have shown that evoked potential signals are in the gamma band range centred at 40 Hz. A recursive digital filter based on [3] is designed to extract data consisting of 40 Hz frequencies only. Using Parseval's theorem, we can obtain the value of 40 Hz power spectrum from the filtered

time-series data. This method has added advantage since it automatically separates VEP from background electroencephalogram (EEG) contamination since EEG is band limited from 0 to 30 Hz. We show experimentally that VEP estimated from this method can be used successfully as features to discriminate between alcoholics and control subjects using a fuzzy ARTMAP classifier.

We extract 400 VEP signals from 10 subjects: five controls and five alcoholics. Measurements are taken for two seconds from 64 electrodes placed on the subject's scalp, which are sampled at 240 Hz. The alcoholics tested have been abstinent for a minimum period of one month and off all medications for the same period of time. The controls are carefully matched for age and are not alcoholics or substance abusers. They are also matched for socio-economic status. The electrode positions are located at standard sites (Standard Electrode Position Nomenclature, American Encephalographic Association). The data is extracted from subjects while being exposed to a single stimulus, which is a picture of an object chosen from the 1980 Snodgrass and Vanderwart picture set [4]. The VEP data is filtered and the 40 Hz power spectra are computed (in time domain) for each channel. A fuzzy ARTMAP (FA) neural network is trained with these 40 Hz spectra to discriminate alcoholics from control (i.e. non-alcoholic) subjects. Our results give an average of 92.5% classification with a maximum of 97% classification.

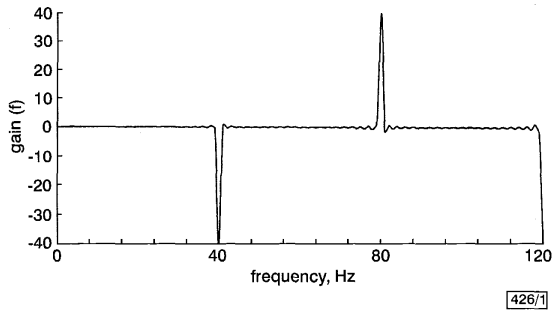

Fig. 1 *Plot of filter gain, $H_1(f)$*

Experimental method: A recursive digital filter is designed with a sampling frequency of 240 Hz. Therefore, 240 zeros are evenly placed around the unit circle in the z-plane. Poles are placed at $\pi/3$ intervals to cancel the zeros at these locations which corresponds to frequencies 0, 40, 80 and 120 Hz. The transfer function for this filter is

$$H_1(z) = 1 - z^{-240}/1 - z^{-6} \tag{1}$$

and the gain of $H_1(z)$ is shown in Fig. 1. The 180° phase shift at 40 Hz is neglected since, in our application, we are interested in power spectrum analysis only. The maximum gain of 40 occurs at pole-zero cancellation angles and the output of the filter is divided with this value. However, our purpose is to extract 40 Hz signal components only, so a bandpass filter with a centre frequency of 40 Hz is designed to remove 0, 80 and 120 Hz signal components. This transfer function of this filter can be expressed as

$$H_2(z) = (1 + z^{-1})^{3n}(1 - z^{-1})^n \tag{2}$$

where the integer n can be increased to reduce the filter bandwidth. We set n = 1 since the 3 dB bandwidth for this case is from 13 to 72 Hz, which is sufficient to significantly remove 0, 80 and 120 Hz frequency components. These filter equations, from eqns. 1 and 2, can be implemented in the time domain by

$$y(i) = [x(i) + x(i-6) + \cdots + x(i-228) + x(i-234)]/40$$
$$\text{and} \quad w(i) = y(i) + 2x(i-1) - 2x(i-3) - x(i-4)/2.28 \tag{3}$$

These equations are obtained with algebraic manipulation and inverse Z transform theory. The maximum gain at 40 Hz for the second filter is $\simeq$ 2.28, which is divided in the second equation to obtain unity gain. The filtered signal, $w(i)$, now contains data components with 40 Hz frequency only. Parseval's theorem can now be used to obtain the 40 Hz power spectrum (PS) of the signal using

$$PS_{40\text{Hz}} = \frac{1}{N}\sum_{i=0}^{N} w^2(i) \tag{4}$$

where N is the total number of data in the filtered signal.

The PS(40 Hz) values of each channel are concatenated into a feature vector and are used by FA to classify the data as alcoholic or control. FA is run with fast learning and voting strategy of 50 simulations. Half of the data is chosen randomly and used to train FA while the rest is used to test the FA network. Further details of FA can be found in [5]. Fig. 2 shows the block diagram of the proposed method.

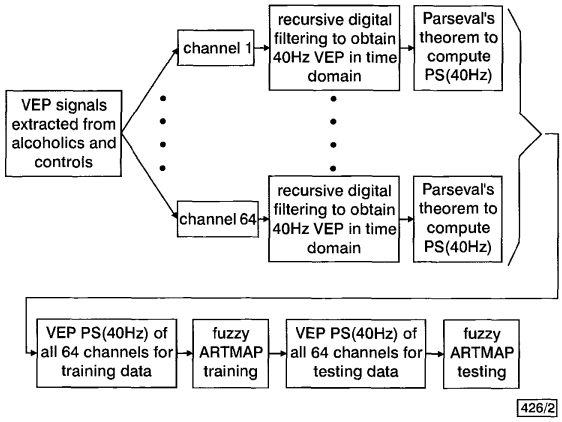

Fig. 2 *Block diagram of proposed method*

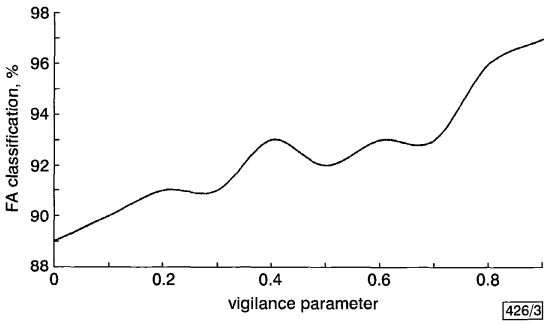

Fig. 3 *FA classification results*

Results: Fig. 3 shows the classification results using FA. The vigilance parameter (VP) of the FA network is varied from 0 to 0.9 in steps of 0.1. The results show that in general, higher VP values give better classification. However, lower VP values enable larger categories to form, leading to broader generalisation and higher code compression, thereby reducing classification time. Overall, the results validate the proposed recursive filter to extract 40 Hz power spectra from VEP to be used as representative features. The highest classification percentage of 97% also shows that 40 Hz VEP is closely related to higher brain functions and reflects the level of focused arousal, which is sufficient to discriminate effectively between alcoholics and control subjects. This would be very useful as a preliminary indicative tool in cases where a person needs to be tested for alcoholism.

Conclusion: We have successfully shown a fast method to extract 40 Hz VEP in the time domain using recursive digital filters, and its use to automate classification of alcoholics from control subjects. In addition, the method eliminates EEG contamination from VEP.

Acknowledgments: We would like to thank H. Begleiter at the Neurodynamics Laboratory at the State University of New York Health Centre at Brooklyn, USA, who generated the raw ERP data and P. Conlon, of Sasco Hill Research, USA, for making the data available to us.

1 May 2001
Electronics Letters Online No: 20010640
DOI: 10.1049/el:20010640

R. Palaniappan and P. Raveendran (*Electrical Department, Engineering Faculty, University Malaya, Kuala Lumpur, 50603, Malaysia*)

References

1 BASAR, E., EROGLU, C.B., DEMIRALP, T., and SCHURMAN, M.: 'Time and frequency analysis of the brain's distributed gamma-band system', *IEEE Eng. Med. Biol. Mag.*, 1995, pp. 400–410
2 BIN, Z., SHENG, Z.Y., ZHONG, Z.L., and YING, H.H.: 'A sliding DFT narrow band filter: extracting 40 Hz EEG'. IEEE EMBS Conf., 1991, Vol. 13, No. 1, pp. 455–456
3 WARIAR, R., and ESWARAN, C.: 'Integer coefficient bandpass filter for the simultaneous removal of baseline wander, 50 and 100 Hz interference from the ECG', *Med. Biol. Eng. Comput.*, 1991, **29**, pp. 333–336
4 SNODGRASS, J.G., and VANDERWART, M.: 'A standardized set of 260 pictures: norms for name agreement, image agreement, familiarity, and visual complexity', *J. Exp. Psychol.: Human Learning and Memory*, 1980, **6**, (2), pp. 174–215
5 CARPENTER, G.A., GROSSBERG, S., and REYNOLDS, J.H.: 'A fuzzy ARTMAP nonparametric probability estimator for nonstationary pattern recognition problems', *IEEE Trans. Neural Netw.*, 1995, **6**, (6), pp. 330–1336

Delay-dependent robust stability of stochastic systems with time delay and nonlinear uncertainties

Dong Yue and Sangchul Won

This Letter is concerned with delay-dependent stability for a class of stochastic systems with time delay and nonlinear uncertainties. A stability criterion, expressed in terms of LMI, is derived based on the Lyapunov-Krasovskii function method and a parameterised model transformation. An example shows that the proposed method is less conservative than alternative methods.

Introduction: Recently, much effort has gone into the development of delay-dependent methods for the stability of uncertain systems with time delay [1 – 10]. Previous studies show that delay-dependent methods generally lead to less conservative results than delay-independent ones. However, to date, most of these have focused on the problem of delay-dependent stability for a deterministic system with a time delay; there are only a few research works [1, 3, 4, 6] on the study of the same problem for a stochastic system with time delay. Moreover, the stability criteria given in [3, 5, 6] are based on matrix norm or matrix measure operations. Unfortunately, these operations usually make the criterion more conservative.

This Letter will address the problem of delay-dependent stability for a class of stochastic systems with time delay and nonlinear uncertainties. To study the stability of the original system, we introduce a parameterised model transformation. Then, an LMI [11] based stability criterion is derived based on the Lyapunov-Krasovskii function.

System description and main result: Consider the following stochastic systems with time delay and nonlinear uncertainties:

$$dx(t) = [Ax(t) + A_1x(t-\tau) + f(t,x(t),x(t-\tau))]dt + g(t,x(t),x(t-\tau))dw(t) \quad (1)$$

$$x(t) = \phi(t) \qquad t \in [-\tau, 0] \quad (2)$$

where $x(t) \in R^n$, A and A_1 are known constant matrices, τ is time delay. Vector $w(t)$ is an m-dimensional Brownian motion defined on probability space, initial condition function $\phi(\cdot) \in C^b_{F_0}([-\tau, 0]; R^n)$, f: $R_+ \times R^n \times R^n \to R^n$ and g: $R_+ \times R^n \times R^n \to R^{n\times m}$ denote the nonlinear uncertainties [4] satisfying

$$\|f(t,x(t),x(t-\tau))\| \le \|G_1x(t)\| + \|G_2x(t-\tau)\| \quad (3)$$

and

$$Trace[g^T(t,x(t),x(t-\tau))g(t,x(t),x(t-\tau))] \le \|G_3x(t)\|^2 + \|G_4x(t-\tau)\|^2 \quad (4)$$

where G_i (i = 1, 2, 3, 4) are known constant matrices of appropriate dimensions.

To analyse the stability of the system described by eqn. 1, we introduce an operator D: $R_+ \times C([-\tau, 0]; R^n) \to R^n$ with

$$D(x_t) = x(t) + B\int_{t-\tau}^{t} x(s)\,ds \quad (5)$$

which is also called the parameterised model transformation [8].

Definition 1: The operator $D(x_t)$ is stable if the exponential mean square stability (EMSS) of the operator $D(x_t)$ implies an EMSS of $x(t)$. In other words, if scalars $\alpha > 0$ and $\beta > 0$ exist such that

$$E\{D^T(x_t)D(x_t)\} \le \alpha \sup_{-\tau\le s\le 0} E\{\|\phi(s)\|^2\}\exp(-\beta t) \qquad t \ge 0 \quad (6)$$

then we can find scalars $\alpha_1 > 0$ and $\beta_1 > 0$ satisfying

$$E\{x^T(t)x(t)\} \le \alpha_1 \sup_{-\tau\le s\le 0} E\{\|\phi(s)\|^2\}\exp(-\beta_1 t) \quad t \ge 0 \quad (7)$$

where $E\{\cdot\}$ is the mathematical expectation. From definition 1, if $D(x_t)$ is a stable operator and satisfies eqn. 6, then we can conclude EMSS of eqn. 1. Next, we give a sufficient condition that guarantees EMSS of eqn. 1.

Theorem 1: Suppose that $D(x_t)$ is a stable operator. For any given $\bar{\tau} > 0$, if there exist positive definite matrices P, T and Q and positive scalars ε_i (i = 1, 2, 3, 4) and ρ such that the following LMIs (eqns. 8 and 9) hold, then the system described by eqn. 1 is exponentially stable in the mean square for any $\tau \in [0, \bar{\tau}]$.

$$\begin{bmatrix} \bar{A}^TP + P\bar{A} + T + \bar{\tau}Q + \rho G_3^TG_3 + (\varepsilon_1 + \bar{\tau}\varepsilon_3)G_1^TG_1 & P\bar{A}_1 & \bar{\tau}\bar{A}^TPB & P & P & 0 & 0 \\ \bar{A}_1^TP & -T + (\varepsilon_2 + \bar{\tau}\varepsilon_4)G_2^TG_2 + \rho G_4^TG_4 & \bar{\tau}\bar{A}_1^TPB & 0 & 0 & 0 & 0 \\ \bar{\tau}B^TP\bar{A} & \bar{\tau}B^TP\bar{A}_1 & -\bar{\tau}Q & 0 & 0 & \bar{\tau}B^TP & \bar{\tau}B^TP \\ P & 0 & 0 & -\varepsilon_1 I & 0 & 0 & 0 \\ P & 0 & 0 & 0 & -\varepsilon_2 I & 0 & 0 \\ 0 & 0 & \bar{\tau}PB & 0 & 0 & -\varepsilon_3 I & 0 \\ 0 & 0 & \bar{\tau}PB & 0 & 0 & 0 & -\varepsilon_4 I \end{bmatrix} < 0 \quad (8)$$

$$P \le \rho I \quad (9)$$

where $\bar{A} = A + B$, $\bar{A}_1 = A_1 - B$ and I is the identity matrix.

Proof of Theorem 1: Construct a Lyapunov-Krasovskii function as

$$V(x(t)) = D^T(x_t)PD(x_t) + \int_{t-\tau}^{t} x^T(s)Tx(s)\,ds + \int_{t-\tau}^{t}\int_{s}^{t} x^T(u)Qx(u)\,du\,ds \quad (10)$$

The weak infinitesimal operator L [3] of the stochastic process $x(t)$, $t \ge 0$, is given by

$$\begin{aligned} LV(x(t)) = {} & 2D^T(x_t)P[\bar{A}x(t) + \bar{A}_1x(t-\tau) + f(t,x(t),x(t-\tau))] \\ & + Trace[g^T(t,x(t),x(t-\tau))Pg(t,x(t),x(t-\tau))] \\ & + x^T(t)Tx(t) - x^T(t-\tau)Tx(t-\tau) + \tau x^T(t)Qx(t) \\ & - \int_{t-\tau}^{t} x^T(s)Qx(s)\,ds \end{aligned} \quad (11)$$

Applying Proposition 2.1 of [9] and noting that $\tau \le \bar{\tau}$ and $P \le \rho I$, we can obtain from eqn. 11 that

$$\begin{aligned} LV(x(t)) \le {} & \int_{t-\tau}^{t} \frac{1}{\tau}\{x^T(t)[\bar{A}^TP + P\bar{A} + P(\varepsilon_1^{-1} + \varepsilon_2^{-1})P \\ & + (\varepsilon_1 + \bar{\tau}\varepsilon_3)G_1^TG_1 + \rho G_3^TG_3 + T + \bar{\tau}Q]x(t) \\ & + 2x^T(t)P\bar{A}_1x(t-\tau) + 2\tau x^T(s)B^TP\bar{A}x(t) \\ & + 2\tau x^T(s)B^TP\bar{A}_1x(t-\tau) \end{aligned}$$